

1D model for the dynamics and expansion of elongated Bose-Einstein condensates

Pietro Massignan* and Michele Modugno†

INFN - LENS - Dipartimento di Fisica, Università di Firenze

Via Nello Carrara 1, 50019 Sesto Fiorentino, Italy

(Dated: November 13, 2018)

We present a 1D effective model for the evolution of a cigar-shaped Bose-Einstein condensate in time dependent potentials whose radial component is harmonic. We apply this model to investigate the dynamics and expansion of condensates in 1D optical lattices, by comparing our predictions with recent experimental data and theoretical results. We also discuss negative-mass effects which could be probed during the expansion of a condensate moving in an optical lattice.

PACS numbers: 03.75.Fi, 05.30.Jp

I. INTRODUCTION

The realization of Bose-Einstein condensates (BECs) in 1D optical lattices provides an important tool to investigate the superfluid and coherence properties of macroscopic quantum systems. Recent experiments have allowed to probe static and dynamic features of these systems such as the Josephson effect [1, 2], the emergence of squeezed states [3], the transition from superfluid to dissipative dynamics [4], Bloch oscillations [5], interference patterns produced by freely expanding condensates [6, 7], and band spectroscopy [8].

These results have stimulated a great interest also from the theoretical point of view, and several models have been proposed to interpret the experimental data. In particular, new analytic results have been derived in the so called “tight binding regime”, based on the assumption that the condensate wave functions in different sites are well separated [2, 6, 9].

A very important point would be to compare these results with the numerical solution of the full 3D Gross-Pitaevskii equation (GPE) that describes the dynamics of BECs at very low temperatures, allowing also for the exploration of the weak binding regime. However, in general the solution of the 3D GPE is a formidable task that suffers severe limitations due to the large memory storage and computational times required to simulate the experimental configurations. To overcome these difficulties the GPE is usually reduced to a 1D equation by means of a static renormalization of the inter-atomic scattering length [10, 11, 12], by using the fact that these systems are effectively one-dimensional. This allows for a realistic description of the trapped axial dynamics, but at the cost of losing any information on the radial degrees of freedom. In general this reduction is indeed too rude, since the transverse dimensions actually play a crucial role both during the expansion, when the 1D constraint is removed, and during the trapped dynamics, where the interplay between the axial and radial components is neces-

sary to account for collective excitations, *e.g.* quadrupole oscillations.

Recently the authors of [13] have proposed an effective 1D wave-equation for BECs confined in cylindrically symmetric potentials, by using a different approach that keeps track also of the transverse dimensions of the condensate. The derivation is based on a variational Ansatz and the wave function of the condensate is factorized in the product of an axial component and a gaussian radial one. The axial wave function satisfies a 1D non polynomial Schrödinger equation (NPSE) that gives remarkable results for the axial ground-state and dynamics of cigar-shaped condensates in cylindrically symmetric traps. However, the derivation in [13] is based on the assumption of a static harmonic radial confinement, and therefore the NPSE is not suitable to study the dynamics under variation of the trapping potential, in particular the ballistic expansion of the condensate after being released from the trap.

In this paper we present a new model that combines the idea of gaussian factorization with the unitary scaling and gauge transformations of [14, 15], allowing for a suitable description of both the transverse and longitudinal evolution of elongated BECs in the presence of a time-dependent harmonic potential plus an arbitrary axial component. The above transformations are used to reabsorb the evolution due to the time variations of the harmonic potential, the latter being replaced by an effective confinement that makes feasible a gaussian factorization even in the case of a sudden release of the external confinement. The evolution of the system is described by an effective 1D GPE that is *dynamically rescaled* (*dr*-GPE) by means of the transformations of [14, 15]. Despite the one dimensional character of this equation, the model is capable to account for the transverse dynamics through an algebraic equation for the radial width coupled to the *dr*-GPE. Therefore this model represents an useful tool to describe both the dynamics and the expansion of BECs in elongated geometries.

The Paper is organized as follows. In Section II we present the derivation of the *dr*-GPE, and in Section III A we discuss its properties in the presence of a pure harmonic potential, by making a comparison with analytical results in the Thomas-Fermi limit. In Section III B

*Electronic address: massignan@lens.unifi.it

†Electronic address: modugno@fi.infn.it

we use the *dr*-GPE to discuss the dynamics and expansion of BECs in the presence of 1D optical lattices, by comparing its predictions with recent experimental and theoretical results [2, 6, 9]. We also present a method to probe negative-mass effects during the expansion of a condensate in the presence of an optical lattice.

II. THE MODEL

We consider a condensate confined in a time-dependent harmonic trapping potential U_{ho} with an additional axial component U_{1D}

$$\begin{aligned} U(\mathbf{r}, t) &= U_{ho}(\mathbf{r}, t) + U_{1D}(r_z, t) \\ &= \frac{1}{2}m\omega_{\perp}^2(t)r_{\perp}^2 + \frac{1}{2}m\omega_z^2(t)r_z^2 + U_{1D}(r_z, t). \end{aligned} \quad (1)$$

The Gross-Pitaevskii equation for the wave-function Ψ of the condensate can be derived from the functional [16]

$$S[\Psi] = \int dt \int d^3\mathbf{r} \Psi^* \left[i\hbar\partial_t + \frac{\hbar^2}{2m}\nabla^2 - U - \frac{gN}{2}|\Psi|^2 \right] \Psi \quad (2)$$

where N is the number of condensed atoms, $g = 4\pi\hbar^2 a/m$ the coupling strength, m the atomic mass and a the inter-atomic scattering length.

In order to account for the time-dependent variations of the confining potential it is convenient to apply the unitary gauge and scaling transform of [14, 15]. Therefore we introduce a rescaled wave function $\tilde{\Psi}(\mathbf{x}, t)$, depending on the rescaled spatial coordinates $x_i \equiv r_i/\lambda_i(t)$ and related to the true wave function $\Psi(\mathbf{r}, t)$ by

$$\Psi(\mathbf{r}, t) = e^{\frac{im}{2\hbar} \sum r_j^2 \frac{\dot{\lambda}_j(t)}{\lambda_j(t)}} \frac{\tilde{\Psi}(\{r_j/\lambda_j(t)\}, t)}{\sqrt{\lambda_1(t)\lambda_2(t)\lambda_3(t)}}. \quad (3)$$

The scaling parameters $\lambda_j(t)$ are solutions of [14]

$$\ddot{\lambda}_j(t) = \frac{\omega_j^2(0)}{\lambda_j(t)\lambda_1(t)\lambda_2(t)\lambda_3(t)} - \omega_j^2(t)\lambda_j(t) \quad (4)$$

with the initial conditions $\lambda(0) = 1$ and $\dot{\lambda}(0) = 0$.

The use of this scaling equations has two advantages: (i) the evolution of $\tilde{\Psi}$ due to the variation of the harmonic trapping potential is mostly absorbed by the scaling and

gauge transform [17] (in the Thomas-Fermi limit $|\tilde{\Psi}|$ is frozen to its initial value); (ii) the rescaled wave function $\tilde{\Psi}$ always evolves in the presence of a fictitious harmonic confinement, that depends on the trapping frequencies at $t = 0$, and therefore the gaussian factorization is applicable even in the case of ballistic expansion, when the real trapping is turned off.

In case of elongated condensates we can obtain a 1D effective model by factorizing the rescaled wave function $\tilde{\Psi}(\mathbf{x}, t)$ in the product of an axial component $\tilde{\psi}(z, t)$ and a gaussian radial component $\tilde{\phi}(x, y, t; \sigma(z, t))$, allowing for an exact integration over the transverse coordinates [12, 13]

$$\tilde{\Psi}(\mathbf{x}, t) = \tilde{\phi}(x, y, t; \sigma(z, t)) \tilde{\psi}(z, t) \quad (5)$$

$$\tilde{\phi}(x, y; \sigma(z, t)) = \frac{1}{\sqrt{\pi}\sigma} e^{-(x^2 + y^2)/2\sigma^2} \quad (6)$$

with the normalization conditions

$$\int dz |\tilde{\psi}(z, t)|^2 = 1 = \iint dx dy |\tilde{\phi}(x, y; \sigma)|^2. \quad (7)$$

With this choice the transverse size of $\tilde{\Psi}$ is characterized by the width $\sigma(z, t)$ that is expected to be a slowly varying function of time, since most of the evolution due to the variation of the trapping potential is absorbed by the unitary transform (3). We note that from Eq. (3) and (5) even the true wave function Ψ can be expressed in the factorized form

$$\Psi(\mathbf{r}, t) = \phi(r_x, r_y, t; \Sigma(r_z, t)) \psi(r_z, t) \quad (8)$$

whose transverse width Σ is given by

$$\Sigma(r_z, t) \equiv \lambda_{\perp}(t)\sigma(r_z/\lambda_z, t). \quad (9)$$

The equations of motion for $\tilde{\psi}$ and σ can be derived by using a variational procedure from the action (2), integrating out the dependence on $\tilde{\phi}$. The problem can be further simplified in the so called ‘‘slowly varying approximation’’, that is when the contribution given by the axial variations of the radial wave function $\tilde{\phi}$ is negligible, $\nabla^2 \tilde{\phi} \approx \nabla_{\perp}^2 \tilde{\phi}$ [13]. In this approximation the action becomes

$$\begin{aligned} S[\Psi] \simeq \int dt \int dz \tilde{\psi}^*(z) \left\{ i\hbar\partial_t + \frac{\hbar^2}{2m} \frac{1}{\lambda_z^2} \nabla_z^2 - \frac{m\omega_z^2(0)}{2} \frac{z^2}{\lambda_z \lambda_{\perp}^2} - U_{1D}(\lambda_z z, t) \right. \\ \left. - \frac{\hbar^2}{2m} \frac{1}{\sigma^2 \lambda_{\perp}^2} - \frac{m\omega_{\perp}^2(0)}{2} \frac{\sigma^2}{\lambda_z \lambda_{\perp}^2} - \frac{1}{2} \frac{gN}{2\pi\sigma^2} \frac{|\tilde{\psi}|^2}{\lambda_z \lambda_{\perp}^2} \right\} \tilde{\psi}(z) \end{aligned} \quad (10)$$

where it is possible to distinguish the contributions of the gaussian integration to the kinetic and potential energy (respectively the terms proportional to $1/\sigma^2$ and σ^2). The requirement of stationarity of this functional yields the

equations for $\tilde{\psi}$

$$i\hbar\partial_t\tilde{\psi}(z) = \left\{ -\frac{\hbar^2}{2m}\frac{1}{\lambda_z^2}\nabla_z^2 + \frac{\hbar^2}{2m}\frac{1}{\sigma^2\lambda_\perp^2} + U_{1D}(\lambda_z z, t) + \frac{1}{\lambda_z\lambda_\perp^2} \left[\frac{m\omega_z^2(0)}{2}z^2 + \frac{m\omega_\perp^2(0)}{2}\sigma^2 + \frac{gN}{2\pi\sigma^2}|\tilde{\psi}|^2 \right] \right\} \tilde{\psi}(z) \quad (11)$$

and for σ

$$\sigma(z, t) = a_\perp \sqrt[4]{\lambda_z(t) + 2aN|\tilde{\psi}(z, t)|^2}, \quad (12)$$

where a_\perp is defined through the harmonic frequency at $t = 0$ by $a_\perp \equiv \sqrt{\hbar/m\omega_\perp(0)}$. From Eqs. (9) and (12), the radial width Σ of the true wave function Ψ is given by

$$\Sigma(r_z, t) = a_\perp \lambda_\perp(t) \sqrt[4]{\lambda_z(t) (1 + 2aN|\psi(r_z, t)|^2)}. \quad (13)$$

By combining Eqs. (11) and (12) we get a 1D nonlinear Schrödinger equation for $\tilde{\psi}$, depending on the parameters λ_j solution of Eq. (4), that we call *dynamically rescaled* Gross-Pitaevskii equation (*dr*-GPE). This equation is energy conserving and requires the same computational effort of a simple 1D-GPE, since the numerical solution of Eq. (4) is straightforward. In the particular case of a time-independent harmonic potential Eqs. (11) and (12) reduce to the NPSE of [13].

The contribution due to the transverse part of the energy, that has been neglected within the approximation $\nabla^2\phi \approx \nabla_\perp^2\phi$, can be estimated by considering the integral

$$\frac{\hbar^2}{2m}\langle |\nabla_{r_z}\phi|^2 \rangle = \frac{\hbar^2}{2m}\frac{\langle |\nabla_z\tilde{\phi}|^2 \rangle}{\lambda_z^2} = \frac{\hbar^2}{2m\lambda_z^2} \int dz \frac{\sigma'^2}{\sigma^2} |\tilde{\psi}|^2 \quad (14)$$

where $\sigma' \equiv \partial_z\sigma$. We have verified that, in the case of a general time-dependent harmonic trapping, the contribution of this term is a negligible fraction of the total energy (less than 0.1%) in a wide range of trap anisotropies ω_z/ω_\perp and number of atoms N . As we show in the next Section, even in the presence of an optical lattice along the axial direction, where the density can show deep modulations on a short scale, the model gives quite accurate results.

In the rest of the paper we consider some applications of the model and make comparisons with analytical results in the Thomas-Fermi (TF) limit, full 3D numerical solutions of the GPE and experimental results, where available. The parameters are chosen in the range of typical experiments at LENS [2, 4, 6]. In particular, we model condensates formed by $2 \cdot 10^4 \leq N \leq 2 \cdot 10^5$ atoms of ^{87}Rb in a cigar-shaped configuration with axial and radial harmonic trapping frequencies respectively $\omega_z = 2\pi \cdot 9$ Hz and $\omega_\perp = 2\pi \cdot 92$ Hz.

To numerically solve the model, we use a Runge-Kutta algorithm for the scaling equations and a FFT split-step method for the *dr*-GPE evolution, mapping the wave function on a discretized lattice [18, 19, 20]. The ground state of the system is found by using a standard imaginary time evolution [16].

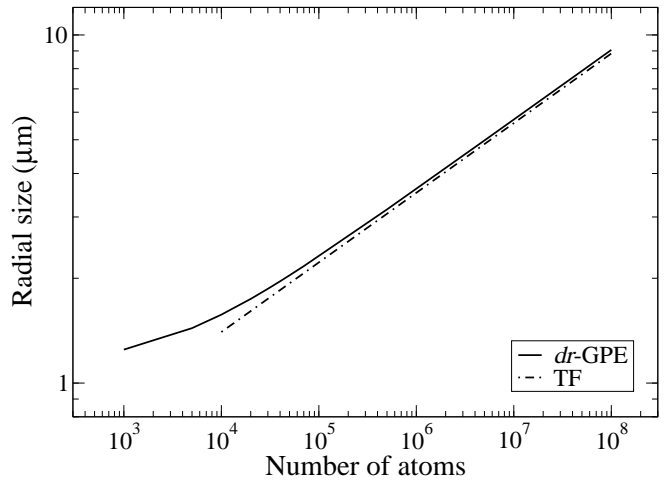


FIG. 1: Comparison of the *dr*-GPE and TF predictions for the radial size of a condensate in a pure harmonic potential as a function of the number of atoms N . The shift between the two curves is expected since the TF approximation truncates the tails of the wave function, leading to a systematic underestimate of the ground state size, especially for small N .

III. APPLICATIONS

A. Harmonic trapping

We start by considering the case of a condensate confined in a pure harmonic potential. As discussed in [13], the ground state axial profile given by the gaussian factorization (5) reproduces the full 3D solution much better than other known 1D model in both the weakly and strongly (TF) interacting regimes. The model also provides reasonable results for the radial profile: the gaussian Ansatz, though slightly overestimating the central density, gives a prediction for the rms radius $R_{rms} \equiv \sqrt{\langle r_\perp^2 \rangle}$ really close to the analytical TF result even in case of very large number of atoms, as shown in Fig. 1.

A remarkable feature of the *dr*-GPE is the possibility to describe the interplay between longitudinal and transverse oscillations induced by modulations of both the axial and radial part of the trapping potential. To illustrate this aspect we consider the low-lying collective excitations induced by a sudden variation of the transverse external confinement. In particular we start with a condensate in the ground state of an anisotropic trap with $\omega_\perp = 2\pi \cdot 92$ Hz and, at $t = 0$, we suddenly switch the transverse frequency to a final value of $\omega_\perp = 2\pi \cdot 80$ Hz, thus inducing shape oscillations involving both the radial and axial directions. For very elongated conden-

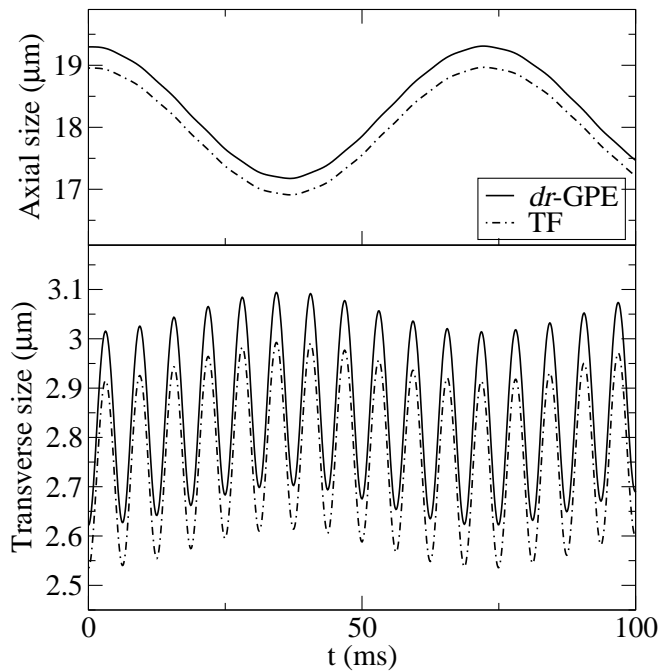


FIG. 2: Evolution of the axial (Z_{rms} , top) and radial (R_{rms} , bottom) sizes of a condensate performing shape oscillations, respectively obtained solving the dr -GPE and the TF Eqs. (4) and (15): in both graphs it is possible to observe the superposition of the quadrupole and the faster transverse breathing frequencies ($N = 2 \cdot 10^5$, $\omega_z = 2\pi \cdot 8.7$ Hz).

sates in the TF regime, these oscillations are characterized by the quadrupole and transverse breathing frequencies, $\omega^Q = \sqrt{5/2}\omega_z$ and $\omega^{TB} = 2\omega_\perp$ respectively [16]. In Fig. 2 we show the behavior of the radial and axial sizes (respectively R_{rms} and $Z_{rms} \equiv \sqrt{\langle z^2 \rangle}$), comparing the dr -GPE predictions with the TF values. The agreement is remarkably good for both the frequency and amplitude of the oscillations; the slight shift between the two curves is expected, due to the truncation of the tails of the wave function in the TF approximation (see Fig. 1). Despite the 1D (axial) character of the dr -GPE, Fig. 2 shows that the equation well mimics the predicted coupling between the axial and radial degrees of freedom. We have checked that the same behavior can be reproduced by changing the axial trapping instead of the radial one, or by using a resonant drive.

Another main difference between our model and any static 1D renormalization of the GPE (1D-GPE) comes out when we consider the ballistic expansion of a condensate suddenly released from the trapping potential. In fact, in the typical experimental regimes the free expansion of a condensate is governed by the TF equations [16]

$$\sqrt{\langle r_i^2 \rangle_{TF}}(t) = \lambda_i(t) \sqrt{\langle r_i^2 \rangle_{TF}}(0) \quad (15)$$

where $\lambda_i(t)$ are solutions of Eq. (4) with $\omega_z(t) = \omega_\perp(t) = 0$. In the case of a 1D GPE a similar relation holds for

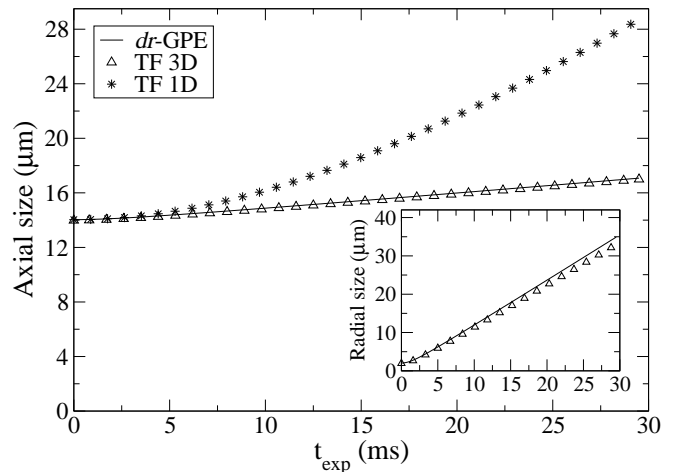


FIG. 3: Axial and radial sizes (respectively Z_{rms} and R_{rms}) of the condensate during a free expansion from a pure harmonic potential, as obtained with the dr -GPE and within the TF approximation in 1D and 3D.

the axial size, except that now the only scaling parameter obeys

$$\ddot{\lambda}_{1D}(t) = \frac{\omega_z^2(0)}{\lambda_{1D}^2(t)} - \omega_z^2(t)\lambda_{1D}(t). \quad (16)$$

One immediate consequence of Eq. (16) is that in the TF limit a 1D GPE equation obtained through a simple renormalization of the coupling constant, although suited to reproduce the (axial) ground state of the system, in general overestimates the repulsive character of the interaction during the expansion. This is shown in Fig. 3 where we plot the axial size of the expanding condensate as obtained from the dr -GPE and the 1D and 3D TF scaling. The nice agreement between the dr -GPE solution and the full dimensional case is due to the use of the scaling equations and to the dynamically reduced nonlinearity of the equation (11) that, in the strongly interacting (TF) limit $aN|\tilde{\psi}|^2 \gg \lambda_z$, takes the form

$$i\hbar\partial_t\tilde{\psi}(z) = \left\{ -\frac{\hbar^2}{2m}\frac{1}{\lambda_z^2}\nabla_z^2 + U_{1D}(\lambda_z z, t) + \frac{1}{\lambda_z\lambda_\perp^2} \left[\frac{m\omega_z^2(0)}{2}z^2 + \frac{3}{2}\hbar\omega_\perp(0)\sqrt{2aN}|\tilde{\psi}| \right] \right\} \tilde{\psi}(z). \quad (17)$$

The inset of Fig. 3 shows that even for the transverse dynamics, despite the 1D character of the dr -GPE, the agreement with the 3D (TF) solution is remarkably good.

B. Optical lattice

We now turn to consider the case of a condensate in a 1D optical lattice. Experimentally this is realized by

means of a retro-reflected laser beam which creates a periodic potential of the form

$$U_{1D}(r_z) = s \cdot E_r \cos^2(2\pi r_z/\lambda_{opt}) \quad (18)$$

where λ_{opt} is the wavelength of the laser, $E_r \equiv \hbar^2/2m\lambda_{opt}^2$ is the recoil energy of an atom absorbing one lattice phonon and s is a dimensionless parameter controlling the intensity of the lattice. Here we chose $\lambda_{opt} = 795$ nm and intensities in the range $0 \leq s \leq 6$ as reported in the experiments [2, 4, 6].

The ground state of the system is characterized by deep periodic variations in the axial density and by pronounced modulations in the radial width, that are well reproduced by our model even for high values of lattice intensities. This is evident in Fig. 4 where we compare the axial density

$$\rho(z) \equiv \langle |\Psi|^2 \rangle_{\perp} = \int d^2 r_{\perp} |\Psi|^2 \quad (19)$$

and the rms transverse radius, integrated only over the radial directions

$$R_{rms}^{\perp}(z) \equiv \sqrt{\langle r_{\perp}^2 \rangle_{\perp}} = \sqrt{\int d^2 r_{\perp} r_{\perp}^2 |\Psi|^2}; \quad (20)$$

with the full 3D solution.

To address the issue of collective excitations we consider both dipole oscillations induced by a sudden displacement of the harmonic potential (here we use $\Delta z = 5 \mu\text{m}$), and quadrupole modes excited as before by changing the harmonic transverse confinement.

Concerning the former, on general grounds one expects a frequency shift which can be explained in terms of a mass renormalization due to the s -dependence of the dispersion relation in the lowest band of the periodic potential [4, 21]: $\omega_z^D \rightarrow \sqrt{m/m^*} \omega_z^D$. In a recent paper it has been predicted, by using a tight binding Ansatz, that the same effective mass m^* can account also for the modification of the quadrupole frequencies [9]: for elongated condensates in the TF regime one expects a linear relationship between the two frequencies, $\omega_z^Q = \sqrt{5/2} \omega_z^D$, independently of the lattice intensity s .

In Fig. 5 we compare the effective mass extracted from the dipole and quadrupole modes with that of a single particle in a periodic potential, near the Brillouin zone center [21]. This picture shows that the predicted relation between ω_z^Q and ω_z^D is very well verified also in the weak binding regime of small s , and that the effects of mean field interaction and of harmonic trapping (both included in the dr -GPE description) give only a minor correction to the single particle picture in a uniform periodic potential. Our results are also in good agreement with a recent experiment realized at LENS [2], as shown in the inset of Fig. 5.

Other interesting features of BECs confined in 1D optical lattices are the interference effects which take place after the removal of the combined optical+harmonic trapping potential. In fact, the free expansion of the system

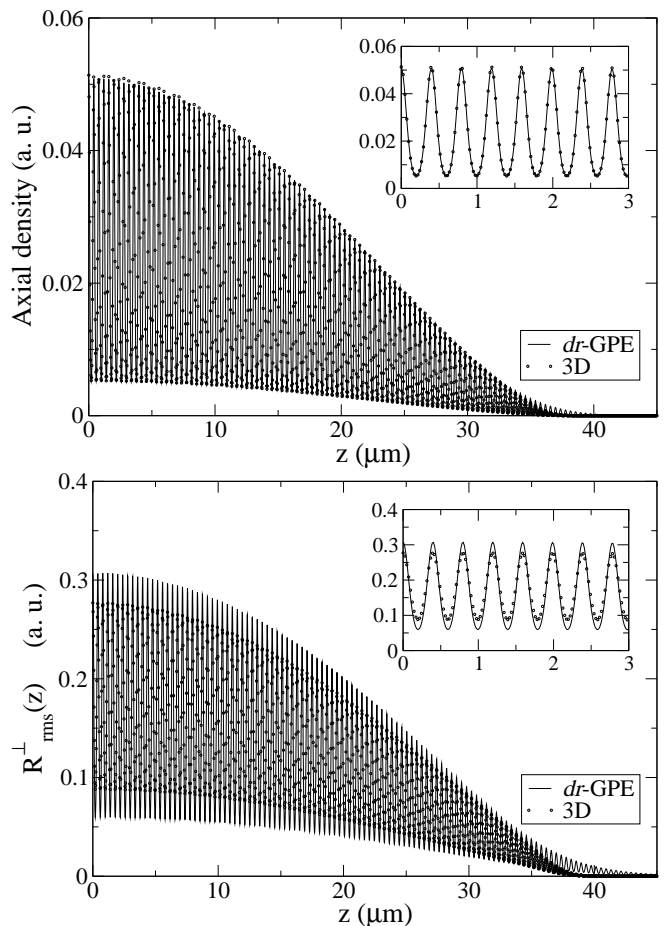


FIG. 4: Axial density $\rho(z)$ (top) and rms transverse radius, averaged only on the transverse coordinates and plotted as function of the axial coordinate (bottom); the insets show the central region of the condensate ($N = 5 \cdot 10^4$, $s = 5$).

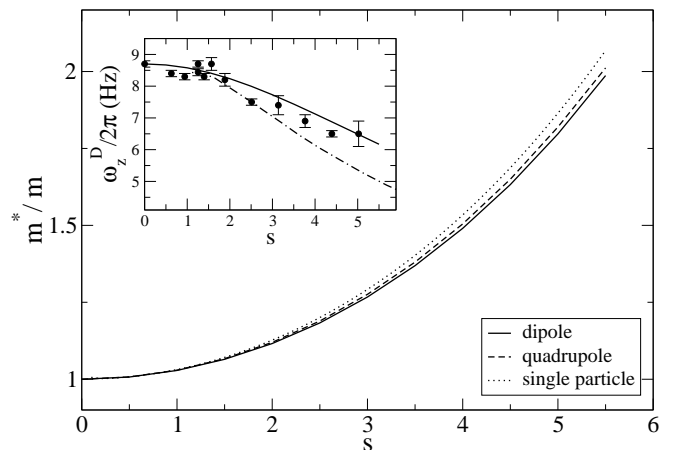


FIG. 5: Effective mass m^* , normalized to the unperturbed value m , as a function of the lattice intensity s , obtained respectively from the dipole (continuous line) and quadrupole (dashed) frequencies, and compared to the case of a single particle in a periodic potential (dotted). In the inset the frequency of the dipole mode is compared with the experimental data and theoretical curve (dashed-dotted) from [2].

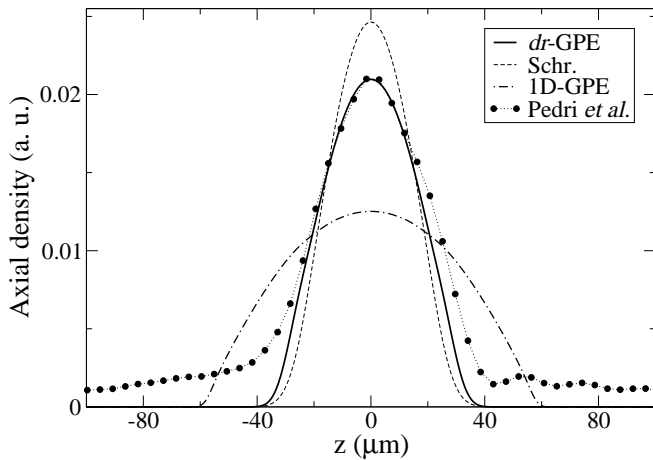


FIG. 6: Axial density of the central peak, as obtained respectively with the dr -GPE, a Schrödinger propagation and the 1D-GPE introduced in [11], compared with the experimental distribution of [6] (the wings are due to the presence of a small thermal component), after $t_{exp} = 29.5$ ms.

causes the single condensates forming the initial array to overlap and leads to the formation of neat interference patterns, showing up as lateral peaks moving with quantized speeds $v_n = \pm n \cdot 2h/\lambda_{opt}m$ (with n integer) [6]. This is essentially a 1D effect, which reflects the momentum distribution of the ground state along the axial direction, and it is well reproduced by our model, regarding both the position and the population of the first lateral peaks. An interesting point concerns the axial expansion of the central peak. A careful analysis of the expanded density profile shows that, compared to other existing 1D equations, the dr -GPE gives a better estimate of the axial size of the central peak. In fact, as can be seen in Fig. 6, a (free) Schrödinger propagation of the ground state underestimates the axial width, while the statically renormalized 1D-GPE introduced in [11], though appropriate to describe the ground state, largely overestimates the axial size after the expansion, as discussed in the previous section. This is indeed due to the fact that the meanfield term of the dr -GPE has a linear character ($\propto |\psi|$, see Eq. 17) which lies between the Schrödinger ($\propto |\psi|^0$) and the GPE ($\propto |\psi|^2$) cases. Our model gives accurate predictions also for the radial expansion of the central peak, which is essentially governed by the TF scaling solution, in agreement with the experimental values and the theory of [6].

We conclude this section by discussing a time-of-flight method that could be used to probe the dispersion relation in the presence of a periodic potential [23], allowing for the investigation of negative-mass effects during the expansion in an optical lattice. The idea is the following: we start with a condensate in the ground state of a pure harmonic potential, and we accelerate it up to a given velocity $v = \hbar q/m$ in the axial direction, *e.g.* by exciting a dipole motion in the harmonic potential. Then we switch off the trap and adiabatically ramp an optical

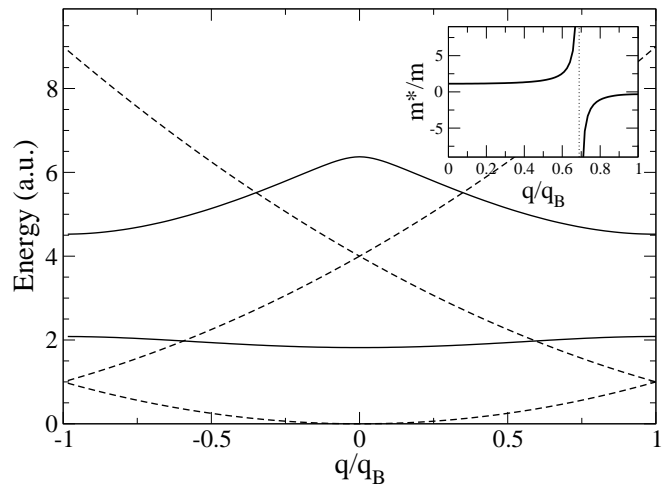


FIG. 7: Structure of the lowest bands for a single particle in a 1D periodic potential with $s = 2$ (solid lines), compared to the free particle case (dashed). The inset shows the behavior of the effective mass m^* , inversely proportional to the band curvature, in the first band for $s = 2$.

lattice along the longitudinal direction up to a desired height s . Here we consider the case of a linear ramp of 15 ms, which is sufficient to ensure the adiabaticity of the process [24] for the velocities considered here. We have indeed verified that applying the reverse ramp after the first one, the additional Fourier components of the wave function at $q \pm 2lq_B$ (with l integer) disappear.

With this procedure we can load the condensate in a Bloch state of axial quasimomentum $\hbar q$ and band index n , and therefore explore effects of effective mass (which depends on s , n and q) far from the Brillouin zone center, during the expansion of the system. In particular, since meanfield effects are ruled out after few milliseconds, the radial and axial expansion are almost decoupled, and the latter can be accounted for by the single particle mass renormalization, as shown in Fig. 7 [8, 21]. The advantage of loading the condensate in the lattice only after the acceleration procedure is that in the reverse case the occurrence of dynamical instability effects prevents the possibility of accelerating the condensate above a critical velocity $v_c < v_B$ [22], where $v_B = \hbar q_B/m = h/m\lambda$ is the Bragg velocity.

In Fig. 8 we show the evolution of the axial size of the condensate during the expansion in the optical lattice, for various initial velocities v . The behavior of the system is essentially determined by the single particle effective mass which characterizes the diffusive (kinetic) term in the evolution equation (as stated before, meanfield effects become negligible after few milliseconds of expansion). Indeed, the figure shows that when q approaches the value $\tilde{q} = 0.6895 q_B$ at which the single particle effective mass for $s = 2$ becomes infinite (see Fig. 7), the expansion in the direction of the lattice gets frozen. For values between \tilde{q} and q_B , m^* becomes negative, and the condensate starts contracting. On the contrary, when

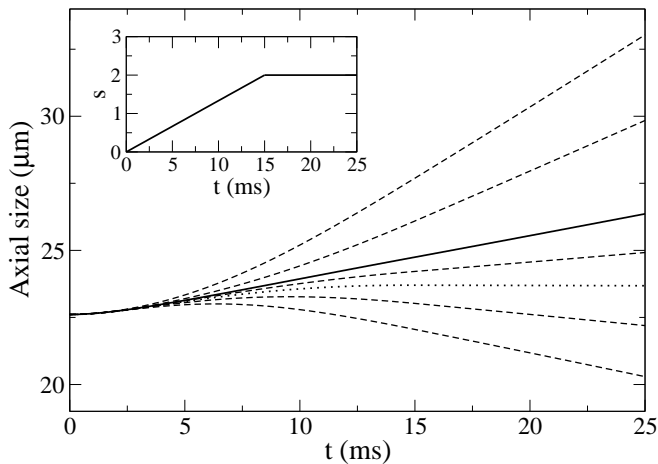


FIG. 8: Evolution of the axial width of a condensate which is loaded during the expansion in a 1D optical lattice, for various velocities: $q/q_B = 1.3, 1.2, 0$ (continuous line), $0.4, 0.685$ (dotted), $0.75, 0.8$, respectively from top to bottom. The lattice intensity is ramped linearly in the first 15 ms of expansion, and then kept fixed at the value $s = 2$ for other 10 ms (see the inset).

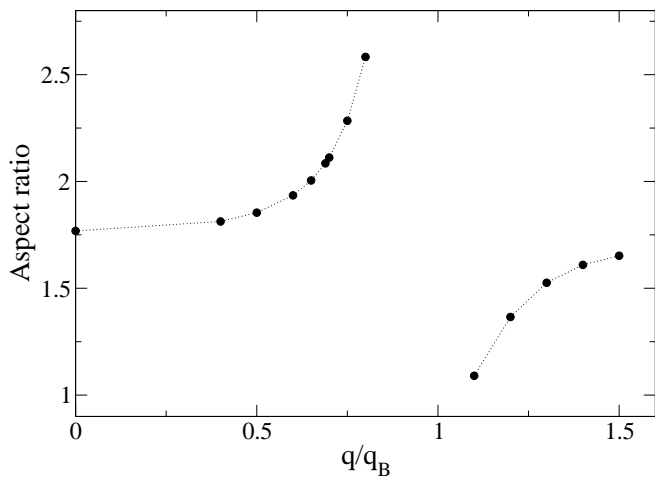


FIG. 9: Aspect ratio after 25 ms of expansion, for a condensate loaded adiabatically in a 1D optical lattice of height $s = 2$, as a function of the condensate velocity.

the condensate is loaded in the second band, that is for $q > q_B$, the expansion is enhanced due to the strong positive curvature near the second band edge.

Since the transverse expansion is only weakly affected by the presence of the lattice, these dramatic effects on the axial expansion can be directly measured on the as-

pect ratio after a fixed evolution time. Indeed, as shown in Fig. 9, the aspect ratio is characterized by a finite jump across the first Brillouin zone boundary, which reflects the discontinuity in the band curvature (the effective mass passes from a negative to a positive value). With the same technique one could probe the band structure also for higher values of q and/or s . In the latter case a longer ramp time could be required in order to ensure an adiabatic loading [24].

IV. CONCLUSIONS

We have presented an effective 1D model for the evolution of an elongated Bose-Einstein condensate in time dependent potentials whose radial component is harmonic, in the presence of an arbitrary axial potential. The model exploits the scaling and gauge transformations of [14, 15], that reabsorb most of the evolution due to the time-dependent variation of the harmonic potential. This makes possible a gaussian factorization for the radial part of the condensate wave function, even in case of a free expansion after the release from the trap.

The evolution of the system is described by a non-linear 1D wave equation (*dr*-GPE) for the axial wave function, dynamically rescaled by means of the aforementioned transformations. Despite the 1D character of the *dr*-GPE, the model also accounts for the radial dynamics of the system, that is necessary to correctly describe collective oscillations and the free expansion of the condensate.

The accuracy of the model has been tested by comparing its predictions with the TF solution in case of pure harmonic trapping and with recent experimental and theoretical results for the dynamics and the expansion of BECs in 1D optical lattices. We have also shown that the quasimomentum dependence of the effective mass has dramatic consequences, which could be easily accessed in the experiments by accelerating and letting expand a condensate in an optical lattice.

Acknowledgments

We are grateful to the group at LENS for providing us with the experimental data and for stimulating discussions. We thank C. Fort for a careful reading of the manuscript. P. M. acknowledges fruitful discussions with N. Piovella and has been supported by the EU under Contract No. HPRI-CT 1999-00111.

-
- [1] B. P. Anderson and M. A. Kasevich, *Science* **282**, 1686 (1998).
 [2] F. S. Cataliotti, S. Burger, C. Fort, P. Maddaloni, F. Minardi, A. Trombettoni, A. Smerzi and M. Inguscio,

- Science* **293**, 843 (2001).
 [3] C. Orzel, A. K. Tuchman, M. L. Fenselau, M. Yasuda and M. A. Kasevich, *Science* **291**, 2386 (2001).
 [4] S. Burger, F. S. Cataliotti, C. Fort, F. Minardi and M.

- Inguscio, M. L. Chiofalo and M. P. Tosi, Phys. Rev. Lett. **86**, 4447 (2001).
- [5] O. Morsch, J.H. Müller, M. Cristiani, D. Ciampini, and E. Arimondo, Phys. Rev. Lett. **87**, 140402 (2001).
- [6] P. Pedri, L. Pitaevskii, S. Stringari, C. Fort, S. Burger, F. S. Cataliotti, P. Maddaloni, F. Minardi and M. Inguscio, Phys. Rev. Lett. **87**, 220401 (2001).
- [7] O. Morsch, M. Cristiani, J.H. Müller, D. Ciampini, and E. Arimondo, preprint `cond-mat/0204528`.
- [8] J. H. Denschlag *et al.*, preprint `cond-mat/0206063`.
- [9] M. Krämer, L. Pitaevskii and S. Stringari, Phys. Rev. Lett. **88**, 180404 (2002).
- [10] M. L. Chiofalo, M. P. Tosi, Phys. Lett. A **268**, 406, (2000); M. L. Chiofalo, S. Succi, and M. P. Tosi, Phys. Rev. E **62**, 7438, (2000).
- [11] M. Trippenbach, Y. B. Band and P. S. Julienne, Phys. Rev. A **62**, 023608 (2000).
- [12] A. D. Jackson, G. M. Kavoulakis and C. J. Pethick, Phys. Rev. A **58**, 2417 (1998).
- [13] L. Salasnich, Laser Physics **12**, 198 (2002); L. Salasnich, A. Parola and L. Reatto, Phys. Rev. A **65**, 043614 (2002).
- [14] Y. Castin and R. Dum, Phys. Rev. Lett. **77**, 5315 (1996).
- [15] Y. Kagan, E. L. Surkov and G. V. Shlyapnikov, Phys. Rev. A **54**, R1753 (1996); Phys. Rev. A **55**, R18 (1997).
- [16] F. Dalfovo, S. Giorgini, L. P. Pitaevskii, S. Stringari, Rev. Mod. Phys. **71**, 463 (1999).
- [17] M. Modugno, L. Pricoupenko and Y. Castin, preprint `cond-mat/0203597` (2002).
- [18] W. H. Press *et al.*, *Numerical Recipes* (Cambridge University Press, N.Y. 1986-92).
- [19] The typical number of lattice sites used is 512 for the dynamics and the expansion in a pure harmonic potential, 4096 for the trapped dynamics in the presence of an optical lattice and 32768 for the expansion of the coherent array of condensates.
- [20] B. Jackson, J. F. McCann and C. S. Adams, J. Phys. B **31**, 4489 (1998).
- [21] N. W. Ashcroft and N. D. Mermin, *Solid State Physics* (Saunders College, Philadelphia 1976).
- [22] F. S. Cataliotti *et al.*, preprint `cond-mat/0207139`.
- [23] M. L. Chiofalo, S. Succi, and M. P. Tosi, Phys. Rev. A **63**, 063613, (2001).
- [24] Y. B. Band, B. Malomed, and M. Trippenbach, Phys. Rev. A **65**, 033607 (2002).